

Received date July 16, 2019; reviewed; accepted date October 29, 2019

## The effect of crosslinking conditions on the dynamic viscosity of organosilicon polymers

Agnieszka Nowacka, Tomasz Klepka

Lublin University of Technology, Faculty of Mechanical Engineering, Department of Technology and Polymer Processing, Nadbystrzycka 36, PL-20618 Lublin, Poland

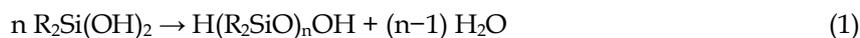
Corresponding author: a.nowacka@pollub.pl (Agnieszka Nowacka)

**Abstract:** This study presents research concerning the development of an organosilicon polymer medium (polymethylhydroborosiloxane), that allows for the optimal selection of viscosity in the medium, for use as an admixture abrasive paste for abrasive flow machining. Based on the results of actual dynamic viscosity medium measurements, the influence of changes in temperature (25 °C, 50 °C and 75 °C) and in the concentration of the crosslinking solution (anhydrite boric acid – 2 wt.%, 4 wt.% and 6 wt.%) were studied. A number of crosslinking medium experiments were carried out, in which the characteristics of storage modulus  $G'$  and loss modulus  $G''$  of the medium containing different concentrations of crosslinking solutions at different temperature were determined. Due to the results obtained, it was possible to select the parameters of the crosslinking solution optimally both in terms of the temperature (50 °C) as well as its concentration (4 wt.%).

**Keywords:** abrasive flow machining, organosilicon polymers, abrasive medium, crosslinking conditions

### 1. Introduction

Organosilicon polymers are an important class of inorganic polymers that find many industrial uses. They are known for their outstanding temperature and oxidative stability, excellent low temperature flexibility, and high resistance to weathering and many chemicals (Dong et al., 2019). These polymers also have a low surface tension and are capable of wetting most surfaces. Organosilicon polymers can be converted into polysiloxanes through the use of hydrolysis technology as expressed by equation 1 or alternatively the disilanol may be converted into cyclic products as expressed by equation 2 (Dobrynin et al., 2019; Dong et al., 2019).



The conversion of the uncured compound into an elastic state through crosslinking – involves the formation of covalent bonds between polymer chains (Din et al., 2018). Depending on the class of organosilicon polymers required, peroxides, anhydrite boric acid, silanes or SiH-containing siloxanes are used for such crosslinking. The crosslinking solution reinforces the elastic silicone network and has a beneficial effect on its rheological properties. The nature, composition and concentration of these crosslinking solutions are critical in determining the properties of the uncured and cured organosilicon polymers (Sun et al., 2019). Crosslinking technology is based on the reaction between Si-OH groups and/or hydrolysable Si-X groups in the presence of moisture (Din et al., 2018; Ao et al., 2018). Depending on the nature of the crosslinking agent, small amounts of acetic acid, amine or neutral by-products such as alcohol are released during curing. At elevated temperatures, anhydrite boric acid decomposes to form highly reactive radicals that chemically crosslink the polymer chains and lead to highly elastic, three-dimensional networks (Kasapgil et al., 2019). For example, peroxide-induced curing is used to produce commercial compounds such as ‘high consistency rubber’ that contains polymers with a high molecular weight and relatively long polymeric chains (Yuan et al., 2019).

A multitude of industry branches (e.g. manufacturing of medical equipment, automotive and aerospace components or mechanical engineering) utilize abrasive suspensions for cutting or finishing high-performance elements (Yadav et al., 2011). Abrasive flow machining (AFM) is an advanced finishing process applied to deburr, polish or angle-grind the edges and surfaces of internal, difficulty-reach workpiece geometries, and it employs specialized viscoelastic abrasive media (Hashimoto et al., 2016; Wang et al., 2018). One of the first studies of this advanced machining process was conducted by Rhoades, who explained its principles in details (Bremerstein, 2015; Garbacz et al., 2008). In abrasive flow machining, two opposing cylinders clamp the workpiece between them and seal the machining passage (Sankar et al., 2018; Wang et al., 2017). Hydraulically operated pistons inside the cylinders repeatedly extrude the abrasive medium back and forth through or across the workpiece until the machining process is finished (Fig. 1). One up-and-down motion of the pistons amounts to a working cycle (Kumar and Hiremath, 2016; Nowacka and Klepka, 2019).

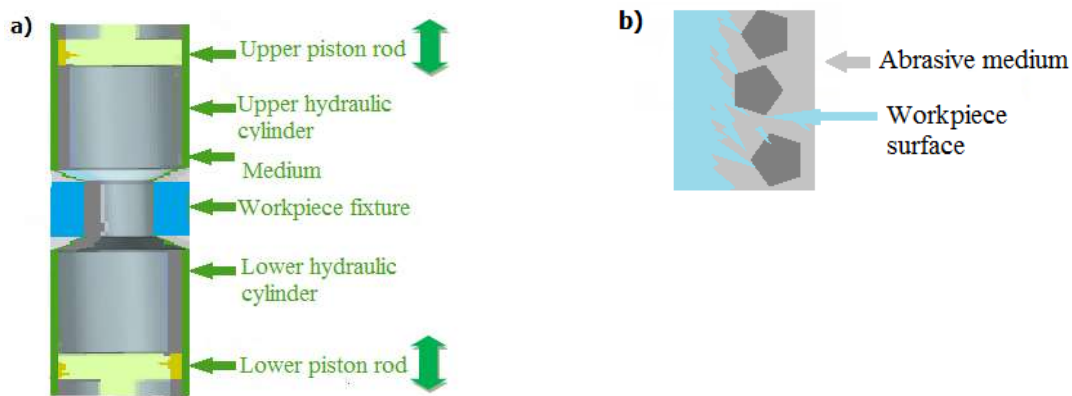


Fig. 1. Process of abrasive flow machining: a) flow of polymer solutions through the object and b) micro-machining of abrasive grains (Nowacka and Klepka, 2019)

The abrasive medium in process abrasive flow machining should exhibit an appropriate rheological behaviour – namely, viscoelasticity (Mao et al., 2019). A viscoelastic medium possesses viscous as well as elastic properties. When it returns to its initial state under very low stress, the medium flows and deforms like a viscous fluid, where a site reacts elastically to rapidly applied and high stress (Meichsner et al., 2016; Sikora and Sasimowski, 2001). This viscoelastic behaviour may be characterized by frequency sweeps in which the rheological properties are measured at high frequencies – rapidly applied stress and low frequencies – gradually applied stress. The results produced by the abrasive media before and after utilization in the machining process are shown in Fig. 2. Storage modulus  $G'$  is regarded as an appropriate way to measure stored deformation energy, while loss modulus  $G''$  is regarded as an appropriate way to measure lost deformation energy. Both moduli represent viscous and elastic deformation behaviour (Toth et al., 2018). The complex viscosity  $\eta^*$  is made up of both moduli and constitutes a measurement for determining the solidity of the sample material (Mezger, 2019).

When material properties only depend on time, but not on the level of mechanical loading, the behaviour of the material is called linear-viscoelastic (Jachowicz et al., 2015; Krasinsiy et al., 2017). Linear viscoelasticity is only precisely defined for a range of infinitesimally small loads. In practice, the validity of the method of measurement for solid polymers is limited to strains of less than 1%, but for polymer melts it can reach 100%. In this case the measurement results express the relationship between strains in the latitudinal ( $\varepsilon_y, \varepsilon_z$ ) and longitudinal ( $\varepsilon_x$ ) directions (Garbacz, 2004; Mezger, 2002). The magnitude of this cross-sectional change is described by Poisson's ratio  $\nu$  (equation 3). In cases of uniaxial loading, it follows that:

$$\nu = -\frac{\varepsilon_y}{\varepsilon_x} = -\frac{\varepsilon_z}{\varepsilon_x} \quad (3)$$

where  $\nu$  is the Poisson's ratio,  $\varepsilon_x$  is the extensional strains in the latitudinal x,  $\varepsilon_z$  is the extensional strains in the latitudinal z,  $\varepsilon_y$  is the extensional strains in the longitudinal y.

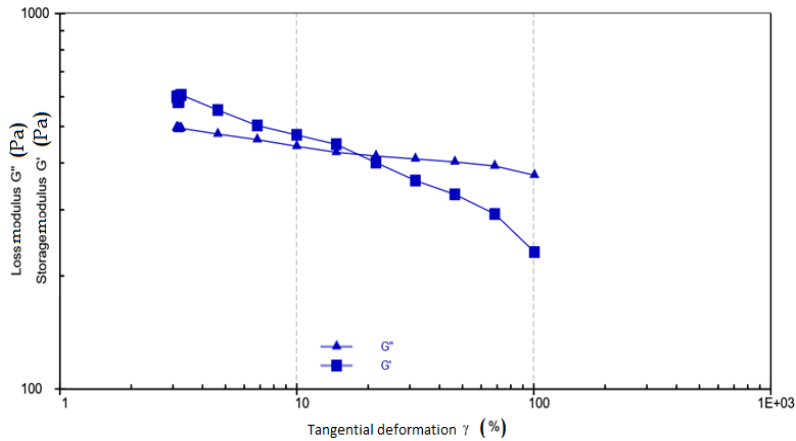


Fig. 2. Results of the frequency sweep – storage modulus  $G'$  and loss modulus  $G''$  as well as complex viscosity  $\eta^*$  are plotted against angular frequency  $\omega$  for the abrasive media before and after utilization (own research)

Linear-viscoelastic behaviour may be expressed by a combination of linear-elastic and linear-viscous processes. Mechanical models may be used for the purposes of demonstration, in which elastic behaviour is symbolized by a spring and viscous behaviour by a dashpot. In the simplest case, the basic elements are both in series, as shown in Fig. 3.

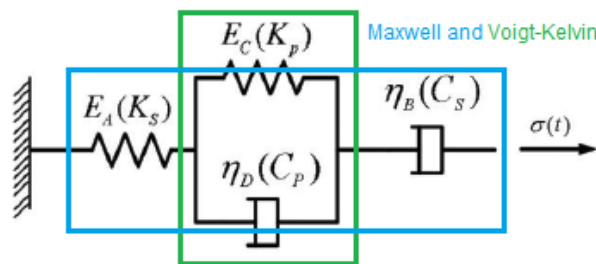


Fig. 3. Analogy model for describing viscoelastic behaviour

The spring and dashpot series is called the Maxwell model. It describes the phenomenon of stress relaxation. In contrast to the Maxwell model, the parallel arrangement of spring and dashpot is known as the Voigt-Kelvin model and it characterizes reaction to a sudden change of stress. Besides the Maxwell and Voigt-Kelvin models, the field of rheology makes use of numerous other rheological models to describe linear-viscoelastic behaviour (Kiljański, 2014; Mezger, 2019). Viscoelastic body distortions ( $\epsilon$ ) – equation 4 – are a function of stress ( $\sigma_0$ ), stress duration ( $t$ ) and the physical properties of the material determined by viscoelastic factors ( $E_A$ ,  $E_C$ ,  $\eta_B$  and  $\eta_D$ ):

$$\epsilon = \sigma_0 \left[ \frac{1}{E_A} + \frac{t}{\eta_B} + \frac{1}{E_C} \left( 1 - \exp\left(-\frac{t \cdot E_C}{\eta_D}\right) \right) \right] \tag{4}$$

where  $\epsilon$  is the extensional strains,  $\sigma_0$  is the zero- tensile stress,  $t$  is the stress duration,  $E_A$  is the elasticity modulus of the first spring,  $E_C$  is the elasticity modulus of the second spring,  $\eta_B$  is the shear viscosity of the first shock,  $\eta_D$  is the shear viscosity of the second first shock.

The value of the  $E_A$  coefficient (equation 5) is equal to the value of the elastic modulus as determined for the initial part of the stretching curve ( $\sigma = \sigma(\epsilon)$ ), therefore it may be determined from the formula where  $\epsilon_{spr}$  represents elastic deformation:

$$E_A = \frac{\sigma}{\epsilon_{spr}} \tag{5}$$

when  $\sigma$  is the tensile stress,  $\epsilon_{spr}$  is the extensional strain elastic deformation.

Values of coefficient  $\eta_B$  are equal to the viscosity values of the silencers placed in series in the adopted model:

$$\eta_B = \sigma \frac{\Delta t}{\Delta \epsilon} = \sigma \frac{t_3 - t_1}{\Delta \epsilon} \tag{6}$$

where  $t_1$  is the initial creeping stage time,  $t_2$  is the creep stage time,  $t_3$  is the creeping stage time,  $\varepsilon_2$  is the creep stage strain,  $\varepsilon_3$  is the creep stage deformation,  $\Delta t = t_3 - t_1$ ,  $\Delta \varepsilon = \varepsilon_{spr} - \varepsilon_3$ .

$E_C$  and  $\eta_D$  values were determined by solving the equations 7 and 8, describing Kelvin-Voight body deformation (where the stress addition and deformation equations are applied). A knowledge of the values of viscoelastic factors ( $E_A$ ,  $E_C$ ,  $\eta_B$  and  $\eta_D$ ) allows for the analysis of changes in stress and strain over time:

$$E_C = \frac{(2\varepsilon_1 - \varepsilon_2)\sigma}{\varepsilon_2^2} \quad (7)$$

$$\eta_D = -\frac{\sigma \cdot t_1 (2\varepsilon_1 - \varepsilon_2)}{\varepsilon_2^2 \ln\left(1 - 2\frac{\varepsilon_1}{\varepsilon_2} + \left(\frac{\varepsilon_1}{\varepsilon_2}\right)^2\right)} \quad (8)$$

Of the four factors describing viscoelastic properties, the most important value of the weld is the  $\eta_B$  value characterizing the irreversible viscous flow. The value of this factor significantly affects the values of deformations in time. With the high value of this deformation factor, the medium is small and the creep of the abrasive medium decreases in practice after a certain time (Hashimoto et al., 2016).

The relationships between chemical structure, molecular relaxation processes and viscoelastic properties are of great practical interest for characterizing and developing materials (Smola, 2010). From the time and temperature dependence of the viscoelastic properties of amorphous polymers, information may be acquired as to their chain stiffness, molecular interaction, molecular weight and molecular weight distribution, crosslink density and molecular orientation, among others (Grellmann and Seidler, 2007; Mezger, 2019; Pei and Friedrich, 2016).

This paper presents an original method for selecting an appropriate temperature and concentration of crosslinking solution for the crosslinking of the organosilicon medium for abrasive flow machining. By using the property of a changing dynamic viscosity, a polymeric medium has been developed that allows for the optimal selection of abrasive medium parameters. The properties of the viscosity medium as an admixture abrasive paste for abrasive flow machining were confirmed during a functional test (Nowacka and Klepka, 2019). The abrasive medium should be characterized by an increased viscosity value as the shear rate increases, a low viscosity value at  $\sigma_0$  (stress value in the initial state). The medium parameters should be determined by  $G' > G''$  and the curves of the moduli should intersect at the high tangential deformation point ( $\gamma$  in %) characteristic of the medium (around  $\gamma > 100\%$ ). Four output variables were optimized: crosslinking temperature ( $^{\circ}\text{C}$ ), concentration of crosslinking solution (wt. %), storage modulus ( $G'$ ) and loss modulus ( $G''$ ).

## 2. Materials and methods

### 2.1. Materials

The test material was a dichlorodimethylsilane (Merck, Germany,  $\geq 98.0\%$ ) and boric acid made by Chempur (Poland,  $\geq 99.0\%$ ). The tested organosilicon polymers were obtained by heating dichlorodimethylsilane with anhydrous boric acid in anhydrous diethyl ether (WarChem, Poland,  $\geq 99.5\%$ ). The anhydrite boric acid was used at concentrations of 2 wt.%, 4 wt.% and 6 wt.%. The crosslinking temperature was 25  $^{\circ}\text{C}$ , 50  $^{\circ}\text{C}$  and 75  $^{\circ}\text{C}$ , respectively. After heating, the reaction mixture was cooled to room temperature and after the boric acid was completely reacted, dichlorodimethylsilane was added, the mixture was cooled to a temperature below 0  $^{\circ}\text{C}$ , then water was added dropwise and the resulting polymethylhydroborosiloxane was separated from the ether layer. The results are shown in Figs. 4 and 5.

### 2.2. Methods

The measurements of the dynamic viscosity experiments were carried out using a Haake Rheometer. The temperature was controlled by a constant temperature plate and the temperature error was  $\pm 0.1$   $^{\circ}\text{C}$ . The temperature plate was set at 23  $^{\circ}\text{C}$ . The rotation rate was controlled by a digitally controlled mechanical cone (C20/ $^{\circ}$ 0.5) controller. The controlled shear stress (CS) measuring system was applied at variable shear stress 0-100 Pa, over a time period of  $t = 180$  s. The Haake rheometer station for the determination of dynamic viscosity in an abrasive medium is shown in Fig. 6. Five replicates of each test were performed. The sets of received test data were checked by a normality test, the chi-square test

( $X^2$ ) was used. In addition, it was determined whether there was a gross error in the resulting set using the Q-Dixon test.

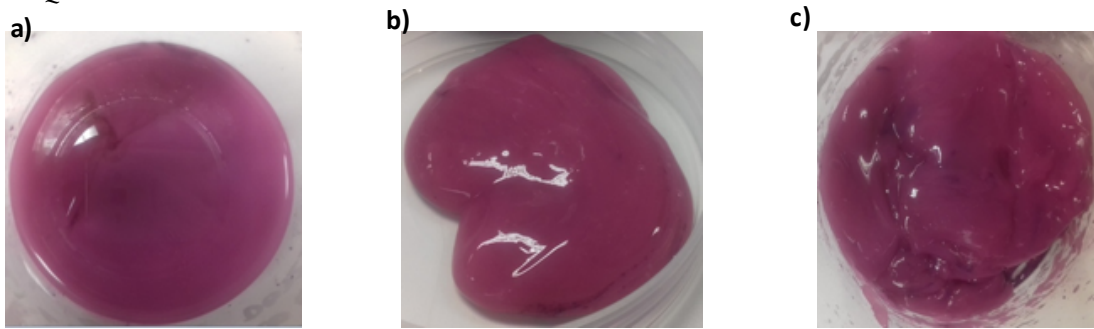


Fig. 4. Polymer medium: effect of the concentration of anhydrite boric acid: a) 2 wt.%, b) 4 wt.% and c) 6 wt.%

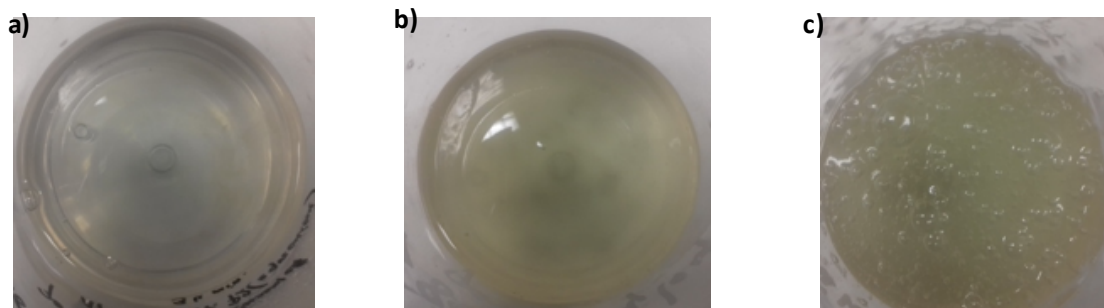


Fig. 5. Polymer medium: effect of crosslinking temperature: a) 25 °C, b) 50 °C and c) 75 °C

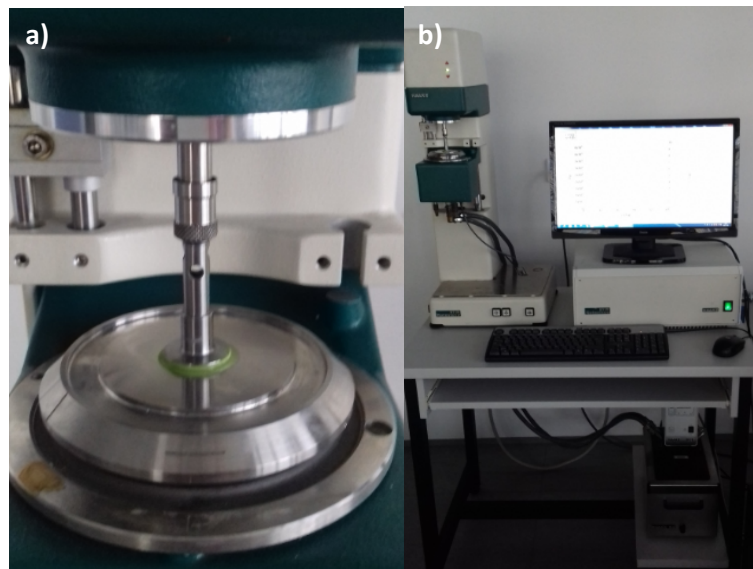


Fig. 6. Haake rheometer station: a) cone-plate system with the medium tested, b) measuring station for the dynamic viscosity at the Department of Polymer Processing

### 3. Results and discussion

#### 3.1. Crosslinking conditions of organosilicon polymers

##### 3.1.1. Effect of crosslinking temperature

In order to investigate the effect of the crosslinking temperature on the crosslinking process efficiency, experiments with three different crosslinking temperature were conducted at a cross-linking time of 180 min, and an agitation rate of 700 rpm. During these experiments, the concentration of the crosslinking solution ( $H_3BO_3$ ) and the mass ratio of anhydrous diethyl ether to dichlorodimethylsilane were kept

constant at 4 wt.% and 2:1, respectively. As shown in Fig. 7, the apparent viscosity efficiency increased when the shear rate was increased up to a value of  $200 \text{ s}^{-1}$ , after which further increases in the shear rate had little effect on the leaching efficiency. The apparent viscosity of the shear rate at  $40 \text{ s}^{-1}$  increased successively as the crosslinking temperature was increased from  $25 \text{ }^\circ\text{C}$  to  $50 \text{ }^\circ\text{C}$ , and finally to  $75 \text{ }^\circ\text{C}$ . The dynamic viscosity increased by no more than 768.4% when the shear of the strain increased from  $70 \text{ s}^{-1}$  to  $200 \text{ s}^{-1}$  after 180 s. In the dynamic viscosity range of 42.09-73.34  $\text{mPa}\cdot\text{s}$ , it showed a slight increase of 12.5% between crosslinking samples with temperatures of  $50 \text{ }^\circ\text{C}$  and  $75 \text{ }^\circ\text{C}$ , and a significant change of 31.4% occurred in the dynamic viscosity for the crosslinking samples between the temperatures of  $25 \text{ }^\circ\text{C}$  and  $75 \text{ }^\circ\text{C}$ . Thus, the viscosity of the dynamic distribution range for the presented sample was in the range of 60.82-73.34  $\text{mPa}\cdot\text{s}$ . In the following experiments, a concentration of 4 wt.% crosslinking solution was adopted.

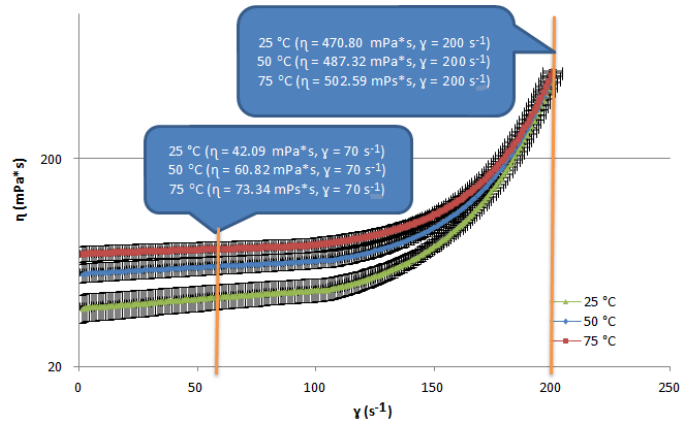


Fig. 7. Viscosity curves of the polymer medium presented on a linear scale

The experiments showed that the storage modulus tended to increase with the decreasing temperature of the crosslinking solution (Fig. 8). The storage modulus  $G'$  has high value that loss modulus  $G''$ . Point 82.6% shear strain is range of intersection  $G'$  with  $G''$ . The  $G'$  decreases in 88% range of the entire curve and  $G'$  changes the value from 12500 Pa to 1500 Pa.

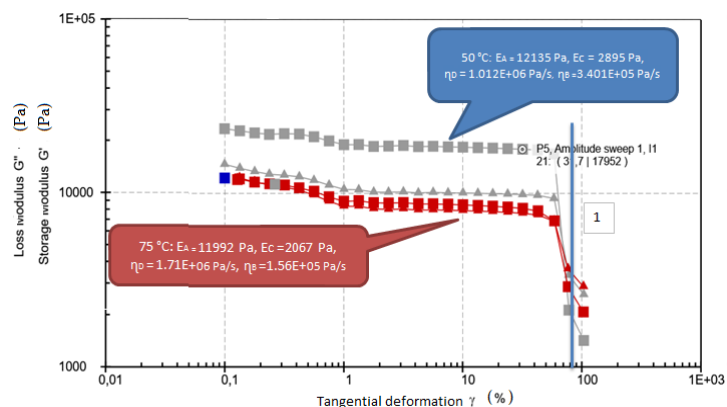


Fig. 8. Amplitude sweep of the medium with a pronounced  $G''$  maximum: 1) macro crack develops throughout the sample up to the intersection point  $G'=G''$ ; after that  $G''>G'$  (fluid state)

It is obvious that the temperature of crosslinking of the medium has a pronounced effect on the structure of the medium, which results in the value of viscosity coefficients  $\eta_B$  (viscosity of the silencer placed in the adopted model). The results are shown in Table 1 (crosslinking temperature:  $25 \text{ }^\circ\text{C}$ ,  $50 \text{ }^\circ\text{C}$  and  $75 \text{ }^\circ\text{C}$ ). Organosilicon polymers possess an inorganic  $(\text{Si-O})$ - backbone similar to silicates which are associated with a high surface energy (Din et al., 2018). The Si-O bonds are strongly polarized and with a lower value temperature of crosslinking of the medium, this should lead to strong intermolecular interactions (Dong et al., 2019). Thus, the temperature of crosslinking of the medium affects the amount of solvent

in the reaction, hydrogen bonds form in the medium to a greater extent at the lower temperature of 50 °C than at 75 °C. A comparison of the maximum distortions of the medium suggested that the values of  $\eta_B$  coefficient differed by 3 orders of magnitude. The maximum coefficient  $\eta_B$  was obtained for a sample crosslinked at 50 °C to a stress ( $\sigma_0$ ) of 30 Pa.

Table 1. Viscoelasticity coefficients for the defined crosslinking temperature solution medium

$\sigma$ (Pa)	0	10	20	30
Temperature (°C)	$\eta_B$ (Pa/s)			
25	$15 \cdot 10^5$	$25 \cdot 10^5$	$38 \cdot 10^5$	$44 \cdot 10^6$
50	$9 \cdot 10^6$	$17 \cdot 10^6$	$50 \cdot 10^6$	$52 \cdot 10^7$
75	$5 \cdot 10^3$	$6 \cdot 10^3$	$11 \cdot 10^3$	$40 \cdot 10^3$
	$\eta_D$ (Pa/s)			
25	429931			
50	434215			
75	490000			
	$E_A$ (Pa)			
25	9831			
50	1734			
75	1073			
	$E_c$ (Pa)			
25	486			
50	1369			
75	1864			

### 3.1.2. Effect of the concentration of the crosslinking solution

While the temperature was maintained at 50 °C, experiments were carried out with three different crosslinking solutions with concentrations of 2-6 wt.%, an agitation rate of 700 rpm and the mass ratio of anhydrous diethyl ether to dichlorodimethylsilane of 2:1, and the influence of the concentration of  $H_3BO_3$  on the dynamic viscosity medium efficiency was evaluated. The results are shown in Fig. 9. It is obvious that the concentration of  $H_3BO_3$  had a pronounced effect on the dynamic viscosity of medium. The experiments showed that the dynamic viscosity of the medium increased with increasing  $H_3BO_3$  concentration, the dynamic viscosity obtained after  $122 \text{ s}^{-1}$  of shear strain could be improved by as much as 11.2 times when the shear strain increased to  $200 \text{ s}^{-1}$ . In the dynamic viscosity range of 12.6-42.60 mPa s, a slight increase of 0.4% for crosslinking samples between the temperature of 50 °C and 75 °C was noted, and a significant change of 30.1% in dynamic viscosity for the crosslinking of samples between the temperatures of 25 °C and 75 °C occurred.

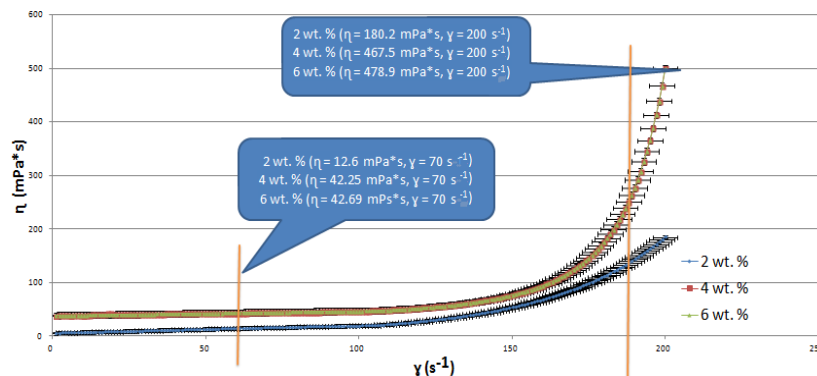


Fig. 9. Viscosity curves of the polymer medium presented on a linear scale

The experiments showed that the storage modulus tended to increase with increases in the concentration of the crosslinking solution (Fig. 10). The storage modulus has a higher range of values than the loss modulus and when the value range of 100-120% shear strain of reaction is reached the structure may be deformed by 31%, at the point where the storage modulus curve intersects with the loss modulus curve from 15500 Pa to 10700 Pa. Data from Fig. 8 indicates that the high concentration of the crosslinking solution resulted in higher storage modulus values. In the storage modulus range of 15500-13500 Pa, the tangential deformation of the medium (6 wt.% solution) at a shear strain value of 100%, reached a high deformation value (32%) and with further changes in the storage modulus range (4 wt.% solution), decrease in tangential deformation occurred after it reached 120%. Summarizing, changes in the storage modulus values as low as 16% were observed. Thus, the desirable storage modulus range (4 wt.% solution) for the presented sample was in the range of 10500-9050 Pa. Due to the low rotation barriers, most of the organosilicon produced was very flexible. Due to the great flexibility of the chain backbone, the activation energy of the viscous flow was very low, and the high concentration of the crosslinking solution resulted in higher storage modulus results (Dobrynin et al., 2019).

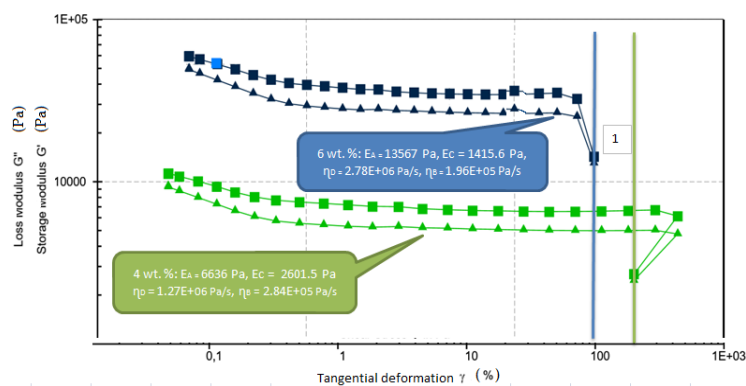


Fig. 10. Amplitude sweep of the medium with a pronounced  $G''$  maximum: 1) macro crack develops after that  $G'' > G'$  (fluid state)

The experiments with viscoelastic coefficients  $\eta_B$  have indicated that these values increased due to the stress ( $\sigma_0$ ) value. The average increase in  $\eta_B$  was 30.7%. The results are shown in Table 2 (crosslinking concentration: 2 wt.%, 4 wt.% and 6 wt.%). The maximum coefficient  $\eta_B$  was obtained for a sample crosslinked at 4 wt.%, at the stress value of ( $\sigma_0$ ) 30 Pa. The most significant increase was observed for the 4 wt.% concentration solution medium – 56.7% from  $\sigma_0$  10-30 Pa. Thus, among the range of mediums in which the rate coefficient  $\eta_B$  increases, the 4 wt.% polymer medium was found to be optimal for abrasive flow machining.

### 3.2. Discussion

In this paper, the process of crosslinking improvement and the study of the effects of dynamic viscosity on organosilicon formation in a medium with various crosslinking temperatures and concentrations of  $H_3BO_3$ , were investigated. Finally, increasing the concentration of crosslinking solution (by 29.65%, 4 wt.%) and the temperature (by 18.73%, 50 °C) results in the desired value of dynamic viscosity with optimum crosslinking parameters. It is very important to verify at what point  $G'$  and  $G''$  intersect for each individual sample, because under these conditions the sample is deformed (Sankar et al., 2018). Apparently, the optimal intersection point of  $G'$  and  $G''$  is 120% for 4 wt.%, and the optimal reaction temperatures are 50 °C and 75 °C for the deformation value of 100% (the effects of these two temperatures are comparable). This is the point at which the internal instantaneous molecular bonds or aggregates are destroyed. At this point there is a lowering of viscosity at increasing shear rate, and a larger part of the energy is irretrievably lost in the form of heat (Wang et al., 2018). This is shown in Figs. 6 and 8. High molecular weight polymers are influenced by the degree of branching of the chain, which is a decisive factor in the processing (abrasive flow machining) of these polymers (Nosál-

Wiercińska et al., 2017; Wang et al., 2017). This depends closely on the rheological behaviour of these polymers and one can expect a correlation between the rheological measurements and the structural elements of individual polymer molecules (Kazmierczak-Rażna et al., 2017; Kumar and Hiremath, 2016). However, the degree of branching of the chain depends on the crosslinking conditions of the polymer (Grochowski et al., 2016; Pei and Friedrich, 2016). The Maxwell and Voigt-Kelvin model describes the viscoelastic properties using four factors. The most important factor is the value of the coefficient  $\eta_B$  characterizing irreversible viscous flow. The value of this factor significantly affects the value of deformations with time (Mezger, 2019). The  $\eta_B$  of the medium may be more than 56.7% (50 °C,  $\epsilon_{30}$ ) and 29.5% (4 wt.%,  $\epsilon_{30}$ ) in comparison to the base  $\epsilon_0$ , which allows to obtain the polymer possessing the desired properties, which offers a higher potential economic value. These results are presented in Tables 1 and 2.

Table 2. Viscoelasticity coefficients for the defined crosslinking concentration solution medium

$\epsilon$ (Pa)	0	10	20	30
Concentration (wt.%)	$\eta_B$ (Pa/s)			
2	$14 \cdot 10^4$	$28 \cdot 10^4$	$34 \cdot 10^4$	$37 \cdot 10^4$
4	$18 \cdot 10^6$	$26 \cdot 10^6$	$44 \cdot 10^6$	$55 \cdot 10^7$
6	$16 \cdot 10^6$	$27 \cdot 10^6$	$42 \cdot 10^6$	$45 \cdot 10^7$
	$\eta_D$ (Pa/s)			
2	429931			
4	434215			
6	$49 \times 10^4$			
	$E_A$ (Pa)			
2	9831			
4	97341073			
6	9734			
	$E_C$ (Pa)			
2	486			
4	1369			
6	1864			

#### 4. Conclusions

Crosslinking conditions have a major influence over the dynamic viscosity of the polymer medium. The dynamic viscosity behaviour indicates that process of crosslinking by the presented medium samples with  $H_3BO_3$  may be described through the temperature and solution concentrations used in the crosslinking medium. By analysing the results of the experiments shown in Figs. 5 and 7, it may be concluded that in order to select the optimal parameters of the crosslinking medium, multiple graphs should be analysed simultaneously. For example, some dynamic viscosity values (for 6 wt.% and 75 °C) reach their highest point, which might seem to be the optimal crosslinking condition. However, it must be taken into account that the 4 wt.% and 50 °C crosslinking conditions of input variables exceed the limits for some output parameters like the storage and loss modulus. Therefore, when analysing the  $\eta_B$  results, one should look for such values of the horizontal axis, for which the dynamic viscosity and modulus parameters ( $\eta$ ,  $\eta_B$ ,  $G'$ ,  $G''$ ), presented on the vertical axis, are as high as possible. Most often, this kind of choice will be a kind of compromise. It may be concluded that the optimal cross-linking conditions with regards to temperature and concentration should not exceed 50 °C and 4 wt.%, respectively. In turn, the storage modulus of the medium should oscillate from 15500 Pa to 12500 Pa, to around 100-120% of tangential deformation. Under these crosslinking conditions, the abrasive medium, dynamic viscosity,  $G'$ ,  $G''$  and  $\eta_B$  values remain at relatively high levels. If we had optimized  $\eta_B$  as 52-

55·10<sup>7</sup> Pa/s (i.e. minimum time required for the deformation), the ideal mixture would have been application of 4 wt.% crosslinking solution and reaction temperature of 50 °C, 6 – 30 Pa.

### Acknowledgments

The authors would like to express their gratitude for the financial support from scholarship for young scientists for the year 2018/2019.

### References

- AO, Y., CAO, K., LIU, B., WANG, P., CHEN, H., HUANG, W., JING, P., ZHAI, M., 2018. *Prohibition of radiation-induced cross-linking of silica-reinforced silicone foam by oxygenation with H<sub>2</sub>O<sub>2</sub>*. Radiat. Phys. Chem. 151, 261-265.
- BREMERSTEIN, T., POTTHOFF, A., MICHAELIS, A., SCHMIEDEL, C., UHLMANN, E., BLUG B., AMANN T., 2015. *Wear of abrasive media and its effect on abrasive flow machining results*, Wear 342-343, 44-51.
- DIN, S., PARKER, S., BRADEN, M., PATEL, M., 2018. *The effects of cross-linking agent and surfactant on the tear strength of novel vinyl polysiloxane impression materials*. Dent. Mater. 34, e334-e343.
- DOBRYNIN, M., PRETORIUS, C., KAMA, D., ROODT, A., BOYARSKIY, V., ISLAMOVA, R., 2019. *Rhodium(I)-catalysed cross-linking of polysiloxanes conducted at room temperature*. J. Catal. 372, 193-200.
- DONG, F., ZHAO, P., DOU, R., FENG, S., 2019. *Amine-functionalized POSS as cross-linkers of polysiloxane containing  $\gamma$ -chloropropyl groups for preparing heat-curable silicone rubber*. Mater. Chem. Phys. 208, 19-27.
- GARBACZ, T., 2004. *Effect of selected auxiliary agents on the properties of surface layer of extruded polyethylene*. Polimery 49, 23-28.
- GARBACZ, T., SAMUJLO, B., 2008. *Selected properties of geometric structure of the surface of cellular polyethylene products*. Polimery 53, 471-476.
- GROCHOWSKI, M., NOSAL-WIERCIŃSKA, A., WIŚNIEWSKA, M., SZABELSKA, A., GOŁĘBIOWSKA, B., 2016. *The effects of homocysteine protonation on double layer parameters at the electrode/chlorates(VII) interface, as well as the kinetics and the mechanism of Bi(III) ion electroreduction*. Electrochim. Acta 207, 48-57.
- GRELLMENN, W., SEIDLER, S., 2007. *Polymer Testing*. Hanser 83-102.
- HASHIMOTO, F., YAMAGUCHI, H., KRAJNIK, P., WEGENER, K., CHAUDHARI, R., HOFFMEISTER, H.W., KUSTER F., 2016. *Abrasive fine-finishing technology*. CIRP Annals – Manufacturing Technology 65, 597-620.
- JACHOWICZ, T., GARBACZ, T., TOR-SWIATEK A., GAJDOŚ, I., CZULAK, A., 2015. *Investigation of selected properties of injection-molded parts subjected to natural aging*. Int. J. Polym. Anal. Ch. 20, 307-315.
- KASAPGIL, E., ANAC, I., ERBIL, H., *Transparent, fluorine-free, heat-resistant, water repellent coating by infusing slippery silicone oil on polysiloxane nanofilament layers prepared by gas phase reaction of n-propyltrichlorosilane and methyltrichlorosilane*. Colloids Surf. A: Physicochem. Eng. Aspects 560, 223-232.
- KAZMIERCZAK-RAZNA, J., NOWICKI, P., WIŚNIEWSKA, M., NOSAL-WIERCIŃSKA, A., PIETRZAK, R., 2017. *Thermal and physicochemical properties of phosphorus-containing activated carbons obtained from biomass*. J. Taiwan Inst. Chem. E. 80, 1006-1013.
- KILJAŃSKI, T., 2014. *Metody pomiaru własności sprężysto lepkich*. Inżynieria i Aparatura Chemiczna 5, 344-346.
- KRASINSKIY, V., SUBERLYAK, O., ANTONUK, V., JACHOWICZ, T., 2017. *Rheological properties of compositions based on modified polyvinyl alcohol*. Adv. Sci. Technol. Res. J. 11, 304-309.
- KUMAR, S., HIREMATH, S. S., 2016. *A review on abrasive flow machining (AFM)*. Procedia Technol. 25, 1297-1304.
- MAO, K., GREENWOOD, D., RAMAKRISNNAN, R., 2019. *The wear resistance improvement of fibre reinforced polymer composite gears*. Wear 426-427(Part B), 1033-1039.
- MEICHSNER, G., MEZGER, T.G., SCHRODER, J., 2016. *Lackeigenschaften messen und steuern*. Vincentz 2<sup>nd</sup> edition, 39-47.
- MEZGER, T.G., 2002. *The rheology handbook*, Vinzenz Verlag, Hannover 81-86, 98-103.
- MEZGER, T.G., 2019. *Applied rheology*, Anton Paar 6<sup>th</sup> edition, 95-112.
- NOSAL-WIERCIŃSKA, A., WIŚNIEWSKA, M., GROCHOWSKI, M., GUZIEJEWSKI, D., FRANUS, W., 2017. *The effect of homocysteine and homocystine protonation on double-layer parameters at the electrode/chlorates(VII) interface*. Adsorpt. Sci. Technol. 35, 396-402.
- NOWACKA, A., KLEPKA, T., 2019. *Zastosowanie polimerów jako mediów ściernych w obróbce przetłoczno-ściernej*. Mechanik 4, 234-237.

- PEI, X.O., FRIEDRICH, K., 2016. *Friction and wear of polymer composites*. Reference Module in Materials Science and Materials Engineering, 1-5.
- SANKAR, M.R., JAIN, V.K., RAJURKAR, K.P., 2018. *Nano-finishing studies using elastically dominant polymers blend abrasive flow finishing medium*. Procedia CIRP 68, 529-534.
- SIKORA, R., SASIMOWSKI, E., 2001. *Polymer cross flow in the screw-based plasticating system*. Polimery 46, 184-191.
- SMOLA, C.M., 2010. *Measurement of rheology and adhesion of pharmaceutical hot melt extrusion*. University of Technology, Graz, 8-15, 27-35.
- SUN, X., CEN, R., GAO, X., LIU, Q., LIU, J., ZHANG, H., YU, J., LIU, P., TAKAHASHI, K., WANG, J., 2019. *Fabrication of epoxy modified polysiloxane with enhanced mechanical properties for marine antifouling application*. Eur. Polym. J. 117, 77-85.
- TOTH, G., NAGY, D., BATA, A., BELINA, K., 2018. *Determination of polymer melts flow-activation energy a function of wide range shear rate*. J. Phys. Conf. Ser. 1045, 012040.
- WANG, C., CHENG, K.C., CHEN, K.Y., LIN, Y.C., 2018. *A Study on the abrasive gels and the application of abrasive flow machining in complex-hole polishing*. Procedia CIRP 68, 523-528.
- WANG, R., LIM, P., HENG, L., MUN, S.D., 2017. *Magnetic abrasive machining of difficult-to-cut materials for ultra-high-speed machining of AISI 304 bars*. Materials 10, 1029-1041.
- YADAV, S.K., SINGH, M.K., SINGH, B.R., 2011. *Effect of unconventional machining on surface roughness of metal: aluminum and brass – a case study of abrasive flow*, J. Phys. Sci. Eng. Technol. 2, 53-60.
- YUAN, Q., CHAI, Z., HUANG, Z., HUANG, Q., 2019. *A new precursor of liquid and curable polysiloxane for highly cost-efficient SiOC-based composites*. Ceram. Int. 45, 7044-7048.